Theor Chem Acc (2017) 136:47
DOI 10.1007/s00214-017-2075-1

REGULAR ARTICLE

Development of a polarizable and flexible model of the hydrated ion potential to study the intriguing case of Sc(III) hydration

Daniel Z. Caralampio[1] · José M. Martínez[1] · Rafael R. Pappalardo[1] · E. Sánchez Marcos[1]

Received: 10 January 2017 / Accepted: 28 February 2017 / Published online: 13 March 2017

Abstract The hydration number of Sc^{3+} aquaion is still an ongoing debate from both experimental and theoretical perspectives, in fact values between 6 and 9 have been proposed. This theoretical study presents the development of Sc^{3+}–H_2O intermolecular potentials based on ab initio potential energy surfaces of two scandium hydrates: $[Sc(H_2O)_6]^{3+}$ and $[Sc(H_2O)_7]^{3+}$. A flexible and polarizable cation and water model has been employed based on the mobile charge density harmonic oscillator (MCDHO) potential. Two classical molecular dynamics simulations of Sc^{3+} in water were carried out with these two new potentials. Data analysis shows very similar results from both simulations: The hydration number obtained is 6 and the average Sc–O distance for the first hydration shell is 2.15 ± 0.01 Å. Estimated hydration enthalpy is very close to the experimental one. The simulated Sc *K*-edge EXAFS spectrum obtained from the structural information provided by the MD simulation agrees fairly well with the experimental spectrum, as well as the main bands of the vibrational power spectra with the IR and Raman spectra.

Published as part of the special collection of articles derived from the 10th Congress on Electronic Structure: Principles and Applications (ESPA-2016).

Electronic supplementary material The online version of this article (doi:10.1007/s00214-017-2075-1) contains supplementary material, which is available to authorized users.

✉ E. Sánchez Marcos
sanchez@us.es

[1] Department of Physical Chemistry, University of Seville, 41012 Seville, Spain

Keywords MP2 · Intermolecular potential · Polarizable and Flexible model · Hydrated ion model · MCDHO2 potential · MD simulation · EXAFS · power spectrum

1 Introduction

The scandium(III) ion in aqueous solution has long been studied without reaching a consensus about its hydration structure at acidic and dilute conditions. Only under these conditions, the aquaion is observed in solution [1]. The more common coordination numbers proposed in the literature are in the range 6–9 [2, 3]. Some evidence proposes the hexacoordination as the most favorable for scandium hydrates. Other studies suggest higher hydration numbers, from 7 to 9, supported by the lability of its hydration shell and its atomic radius, in between Al^{3+} hexacoordinated aquaion, and the closest heavy trivalent cation of its group, Y^{3+}, whose aquaion is an octahydrate [4].

Pioneering Raman studies by Kanno et al. [5] discarded the octahedral symmetry comparing the absorption bands with the well-established case of the hydrated aluminum. A combined XRD and EXAFS study by Yamaguchi et al. [6] found a Sc–O distance of 2.18 Å and a coordination number of 7. However, a more recent Raman and quantum mechanics (QM) study [2] carried out by Rudolph and Pye, supported the octahedral geometry of $[Sc(H_2O)_6]^{3+}$ in $Sc(ClO_4)_3$ solution where it has been proved that the counterion does not penetrate the first shell. Smirnov et al. [7, 8] observed by means of X-ray diffraction a decreasing coordination with temperature, with a seven coordination at 25 °C for a 1 M $Sc(ClO_4)_3$ solution and an aquocomplex with six water molecules and one chloride for a 1 M $ScCl_3$ solution.

Rode et al. [9] studied the Sc(III) hydration using molecular dynamics (MD) simulations at different levels.

Classical MD simulations with or without 3-body corrections led to a coordination 7.8–9.0 and Sc–O distance 2.27–2.10 Å. When they used a hybrid QM/MM method including one or two shells in the QM part of the system a heptacoordination with Sc–O distance of 2.14–2.15 Å was obtained.

A QM study [10] about the water exchange on the aquaions of the *d*–series concluded that the water exchange proceeds via an associative mechanism for the scandium aquaion and sets the hexahydrate more stable than the heptahydrate, but both coordinations could coexist in solution.

The groups of Persson and Sandström [11–13] used crystal compounds including hydrates with different coordination numbers as references to compare with aqueous solutions containing Sc^{3+}. The samples were studied by EXAFS and LAXS techniques, proposing an aquaion bearing six water molecules at 2.17 Å and one or two additional water molecules in apical positions, 2.32–2.5 Å, although experimental resolution precludes to assign the number of them unambiguously. The lack of a splitting in the pre-edge on the Sc *K*-edge XANES in the aqueous solution sample which is observed in the solid sample of the octahedral hydrate scandium salts is invoked by these authors to support a coordination higher than six [14].

Migliorati and D'Angelo have very recently carried out a MD-EXAFS study [3] finding an octahydrate with a broad Sc–O peak formed by six water molecules at 2.16 Å, two additional water molecules at 2.26 and 2.31 Å, and one apical molecule in a meso-shell [15] placed between 2.9 and 3.7 Å. This result is supported by the EXAFS analysis, where a good agreement for an octa-coordination with an average distance of 2.19 Å was obtained.

The aim of this work is to get insight into the ongoing debate on Sc^{3+} hydration number. To fulfill this aim we have built an ab initio intermolecular potential based on the hydrated ion approach developed by our group [16–18], but improved by the use of a polarizable and flexible water model. Two hydrates of coordination six and seven are chosen as reference to build the QM potential energy surface to be fitted. The available experimental EXAFS spectrum [11] will be compared with the simulated one derived from the MD simulation structural information.

2 Methodology

2.1 Intermolecular potential

The basic idea of the hydrated ion (HI) model is the recognition that the species interacting in aqueous solution is the metal cation surrounded by a given number of water molecules [4]. The statistical implementation of the (HI) model was proposed to deal with stable aquaions, then $[M(H_2O)_n]^{m+}-H_2O$, hydrated ion-water (HIW) interaction potential was built [16, 18]. A second potential $[M-(H_2O)_n]^{m+}$ was needed to describe the intrinsic aquaion dynamics, the IW1 (ion-water 1st shell) potential [17, 18]. This methodology was applied to a wide set of stable aquaions, e.g., M = Cr^{3+}, Ir^{3+}, Rh^{3+}, Al^{3+}, Mg^{2+}, Be^{2+}, Pd^{2+}, Pt^{2+} [15, 18, 19]. The limitation of this approach is that first-shell water molecules are different from those of bulk. That is, water exchange is not allowed during the simulation. To overcome this shortcoming of our original HI model, we developed a methodology allowing the exchange of water molecules from the first shell to the bulk [20, 21]. The ion and the water molecule were defined by means of a polarizable and flexible model, the mobile charge density harmonic oscillator (MCDHO) potential developed by Ortega-Blake et al. [22] on the basis of a mobile charge density joined to the nuclei by a harmonic oscillator. The basic idea is to develop the IW1 potential in the framework of a polarizable and flexible water model, allowing deformation and elongation of the aquaion geometry larger than those considered in the original IW1 methodology [17]. This exchangeable HI potential has been already applied to the description of trivalent lanthanoid and actinoid cations aqueous solutions [20, 21, 23], as well as to the monovalent cations of the alkaline group [24]. In this work, we have applied the exchangeable HI potential to a stable aquaion, $[Sc(H_2O)_n]^{3+}$, using a reduced prospection of the potential energy surface. Figure 1 presents the type of structures chosen and the corresponding deformation followed. The use of $[Sc(H_2O)_n]^{3+}$ aggregate as the reference structure to extract the ion-water interaction potential implies that in the QM interaction energy many-body terms up to $(n-1)$th order are implicit. In this study we will focus our development on two aquaions which have been taken as alternative references to build two different site–site Sc^{3+}–H_2O potentials, the hexa- and the hepta-hydrated aquaion, hereafter called *POT*6 and *POT*7, respectively. Nevertheless, once provided that n is greater than a given value which allows the inclusion of the main many-body contributions, the potential behavior must be quite similar regardless the n value taken to build the potential. To check this point, we have developed two additional potentials based on $n = 4$ (*POT*4) and $n = 8$ (*POT*8). Results are given in Supplementary Material (SM), Figure S4, and both of them lead to results very similar to those obtained with *POT*6 and *POT*7. A modified version of MCDHO water model recently proposed, MCDHO2 [25], was chosen as it gives a better description of liquid water mobility.

The general expression of the exchangeable HI potential is given in the SM, together with the set of coefficients obtained for *POT*6 and *POT*7. A plot showing the goodness of fit is also included in SM. The typical

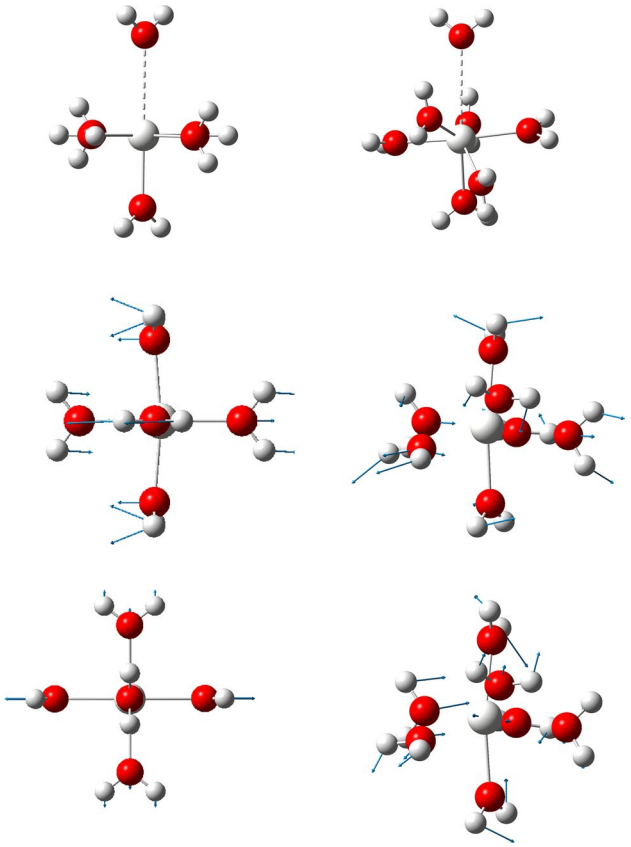

Fig. 1 Representative set of structures chosen from Sc^{3+} hexahydrate and heptahydrate used to build the intermolecular potentials *POT*6 (left) and *POT*7 (*right*). *Arrows* indicates the type of distortion (normal mode) considered in the hydrates. From *top* to *bottom* shortening and lengthening of only one H_2O to the central cation, bending mode and asymmetric stretching mode

deviations of these fits are 0.77 and 1.29 kcal/mol for *POT*6 and *POT*7, respectively. It is worth pointing out that for previous fitting of the (HIW+IW1) potentials of stable aquaions, which used non-polarizable models, the number of structures included in the fitting was close to 1000. In this case, only 40 structures are needed to get reliable potentials. Such a low number of structures for sampling should not be surprising because in each distorted $[Sc(H_2O)_n]^{3+}$ cluster considered there are implicitly n Sc–H_2O interactions corrected from $(n-1)$-body contributions. Therefore, 280 Sc–H_2O interactions, including many-body corrections up to sixth-order were considered in the *POT*7 development.

2.2 Computational details

QM calculations at the second order Moller-Plesset level with the aug-cc-pVTZ basis set for oxygen and hydrogen and the Stuttgart pseudopotential with the recommended basis set for the Scandium [26] were carried out to prospect the potential energy surface of the hexahydrate and the heptahydrate. Computations were carried out with the Gaussian 09 package [27].

Two molecular dynamics (MD) simulations were run for a system formed by 1 Sc^{3+} and 1000 MCDHO2 water molecules at 300 K in the canonical ensemble. Boxlength (31.1 Å) was set up to reproduce the liquid water density at this temperature. In one of them, *POT*6 was used to describe Sc^{3+}–H_2O interactions, whereas in the second one *POT*7 was employed. The Noose-Hoover thermostat with a relaxation time of 0.5 ps and the Ewald sum for electrostatics were employed. The polarizable character of the particle was described by an adiabatic shell model. A timestep of 0.1 ps was needed to describe the high-frequency moves. A modified version of DLPOLY code [28] incorporating the force field used (see SM) was employed. An equilibration period of 150 ps was run before the production time. 1 ns simulation time was analyzed in each simulation. Longer simulation runs up to 5 ns were carried out to check the Sc(III) hexahydrate stability and the convergence of the present results for the case of *POT*6.

2.3 Simulated EXAFS spectrum

K-edge Sc experimental EXAFS spectra from $Sc(ClO_4)_3$ solution corresponds to the work of Lindqvist-Reis et al. [11]. Simulated *K*-edge EXAFS function has been built averaging the signal of 500 evenly distributed snapshots. Scandium, oxygen and hydrogen atoms were considered in the calculation of the backscattering potential and considering only the ion and oxygen atoms in the calculation of the scattering paths using the FEFF 9.6 code [29]. The Hedin-Lundqvist exchange-correlation potential was used to compute the electron density distribution within the SCF approach. FEFF input files for the EXAFS calculations are given in SM. The cutoff radius used to select the extension of the hydration water shell around the Sc absorber atom was large enough to include well beyond the second hydration shell ($R_{cut} = 8$ Å, see RDF in Fig. 2). ΔE_o applied for the simulated EXAFS spectrum was chosen such as it matches the first EXAFS oscillation (3–5 $Å^{-1}$). Previous examples of the methodology applied to others highly charged metal cations in water can be found elsewhere [20, 21, 30, 31].

3 Results

3.1 Clusters

Table 1 checks the behavior of the developed potentials to predict the interaction energies (E_{int}) of several scandium hydrates at different geometries in the gas phase. The upper part of the table compares the QM and the *POT*6 E_{int} for

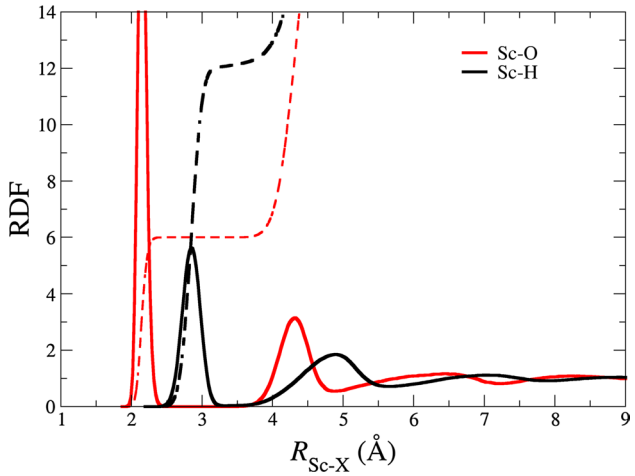

Fig. 2 Sc–O and Sc–H RDF (*solid lines*) and their corresponding coordination number (*dashed lines*) for the MD simulation derived from the use of POT6 intermolecular potential

several optimized geometries of $[Sc(H_2O)_n]^{3+}$. The lower part of the table corresponds to the QM and *POT7* comparison. The column headers A//B denotes A for the method used to compute E_{int} and B for the geometry optimization method. To facilitate the comparison of the MP2 results (MP2//MP2) which are the ab initio energy references for the fitting potentials, this column is repeated for *POT6* and *POT7* results. The agreement of E_{int} clusters provided by the two potentials at the MP2 geometries is satisfactory, the mean error being less than 2% (see *POT6*//MP2 and *POT7*// MP2 columns). Both potentials show the trend to favor the clusters where a seventh or eighth water molecule is placed in the second shell instead of remaining in the first shell. This is also the MP2 behavior and was already found by Rudoplh and Pye [2] for a set of Sc^{3+} hydrates at the MP2 level. When the examined structures are those optimized with *POT6* and *POT7* the preferred cluster with eight solvent molecules is a hexahydrate with two water molecules in the second shell (see *POT6*//*POT6* and *POT7*//*POT7* columns). The comparison between the clusters optimized by the two potentials as well as using the MP2 geometries shows that *POT7* is a more attracting potential than *POT6* by ~15 kcal/mol. However, the optimized geometries of the different clusters are very similar as can be verified by E_{int} values provided by the MP2 single points on the geometries optimized by *POT6* or *POT7*. (*cf*. MP2//*POT6* vs. MP2//*POT7*).

Table 2 collects the average Sc–O distance of the hexa- and hepta-hydrates obtained when the QM MP2 level is used under two conditions, isolated or in a cavity immersed

Table 2 Sc–O distance (Å) of the hexa- and heptahydrate optimized structure for the MP2 level in gas phase and in a dielectric continuum (PCM), and for the two potentials developed

Structure	MP2// MP2	MP2 (PCM)// MP2 (PCM)	*POT6*//*POT6*	*POT7*//*POT7*
6	2.175	2.143	2.175	2.168
7	2.230	2.205	2.253	2.240

Table 1 Interaction Energy, E_{int} (kcal/mol) of different structures of Sc^{3+} hydrates derived from the QM calculations and the interaction potentials developed in this work

Structure	MP2//MP2	*POT6*//MP2	*POT6*//*POT6*	MP2//*POT6*
POT6				
6	−539.3	−539.3	−543.1	−535.5
6+1	−574.2	−566.8	−576.5	−569.1
7	−570.5	−554.7	−559.7	−565.2
7+1	−606.2	−585.4	−606.5*	−601.2*
8	−601.0	−573.9	−607.4*	−605.8*
Structure	MP2/MP2	*POT7*/MP2	*POT7*/*POT7*	MP2/*POT7*
POT7				
6	−539.3	−554.1	−557.9	−535.6
6+1	−574.2	−580.6	−591.3	−569.1
7	−570.5	−570.5	−575.2	−565.4
7+1	−606.2	−601.6	−621.5*	−601.2*
8	−601.0	−590.6	−622.5*	−605.6*

The first acronym refers to the energy calculation and the second one after the // symbol the method employed to optimize the geometry

* 6 + 2 structure

in a continuum dielectric, which is described by the PCM model [32]. The table also collects the distances supplied by the optimized structure with *POT*6 and *POT*7. The hexahydrate under solvation effect introduced by the PCM approach has a distance of 2.14 Å, close to the experimental range of the aqueous scandium studies 2.15–2.18 Å, meanwhile the heptahydrate has a longer average interatomic distance 2.21 Å. As noted with E_{int} values, *POT*6 and *POT*7 give distances very close to their QM references and the difference with the distance of the hydrate for which it has not been fitted is only ~0.01–0.02 Å.

3.2 MD simulations

Figure 2 shows the Sc–O (red lines) and Sc–H (black lines) radial distribution functions (RDF) obtained from the simulation using *POT6*. Running coordination numbers are also included in the figure. The corresponding RDFs obtained from the simulation using *POT7* are very similar to the function plotted in the figure, then it has not been included, but the most representative structural parameters have been incorporated into Table 3. The first conclusion is that Sc^{3+} aquaion is a very stable hexahydrate, predicted by both *POT*6 and *POT*7: a well-defined and narrow Sc–O peak centered at 2.15 Å is observed in the RDF which integrates to 6. It is worth pointing out that the hexacoordination is also predicted by the MD simulation where the Sc–H_2O intermolecular potential was built from the hepta-hydrated structures. There is a depletion zone in the intermediate region, 2.5–3.7 Å, between the first and the second hydration shells, which indicates that no exchange between these shells took place during the 1 ns simulation time. In Table 3, the main structural and dynamical results for the *POT*6 and *POT*7 MD simulations are collected. The Sc–H first peak is very well-defined and centered at 2.85 Å. The gap of 0.7 Å with respect to the corresponding Sc–O first shell and the tilt angle of the water molecules in this shell, ~20°, indicate that these water molecules are arranged following an ion–dipole orientation. The depletion zone after the first peak in the Sc–H RDF confirms the stable character of Sc^{3+} aquaion, a hexacoordinated hydrate. The consistency of this aquaion leads to promote a very well-defined second hydration shell, where the Sc–O peak is centered at 4.3 Å and the Sc–H one at 4.9 Å, with 13–14 water molecules. Differing from the first shell, beyond the second peak the RDF minimum does not go down to zero but to 0.6, implying a significant second shell-bulk water exchange. First-shell Debye-Waller factor, DW, computed as the average of the mean-square displacements of $R(\text{Sc–O})_I$, $[\sigma_I^2 = \langle(R_I - \overline{R_I})^2\rangle]$, provides a value within the range of the experimental DW values obtained in the literature. The water molecule polarization in the two hydration shells is quantified by the dipole moment: A strong polarization in the first-shell, 4.6 D, with respect to the water molecule bulk value, 2.9 D is observed. Such a high dipole moment has a double origin. First of all the short ion-water distance for this trivalent cation, 2.15 Å, compared to the trivalent lanthanoid ions, where the distances are in the 2.35–2.55 Å range, and the first-shell water molecule dipole moment are in between 3.3 and 3.95 D [25, 33]. Second the metal-first-shell water molecule charge transfer is significant for this cation, but it is not included explicitly in the interaction potential. The charge transfer is then compensated by a strong interaction leading to a higher polarization of the first-shell water molecules. Second hydration shell still exhibits polarization effects as its value is 3.2D.

Table 3 Main results obtained from MD simulations using *POT*6 and *POT*7 and comparison with experimental and theoretical published values

Property	*POT*6	*POT*7	Literature
$R(\text{M-O}_I)$ (Å)	2.145	2.140	2.15–2.18 [9, 11]
$\overline{R(\text{M-O}_I)}$ (Å)	2.155	2.148	–
CN_I	6	6	6–8 [3, 7, 9, 11]
DW (Å^2)	0.0039	0.00371	0.003–0.012 [3, 11]
$R(\text{M-H}_I)$ (Å)	2.85	2.84	–
CN_{II}	12.1	12.1	–
$\overline{R(\text{M-H}_I)}$ (Å)	2.85	2.84	2.82–2.86 [3, 9]
tilt angle$_I$ (degrees)	21	22	11–10 [9]
μ ($(H_2O)_I$) (Debye)	4.6	4.6	–
$R(\text{M-O}_{II})$ (Å)	4.32	4.30	4.10–4.27 [7, 11]
CN_{II}	13.5	13.7	13
$R(\text{M-H}_{II})$ (Å)	4.90	4.90	4.99–5.04 [9]
tilt angle$_{II}$ (degrees)	52	52	–
μ($(H_2O)_{II}$) (Debye)	3.2	3.2	–
MRT (ns)	> 1	> 1	10 [34]
ΔH_{hyd} (kcal/mol)	−909	−925	−948.1 [35]
Diffusion (10^{-5} cm^2/s)	0.24	0.23	0.574 [36]

Regarding water molecule residence times (MRT), the only available experimental datum was given by Merbach and Helm [34], 10 ns. Since our simulation time was 1 ns and no exchange was observed, only we can state that MRT value is greater than 1 ns. Translational diffusion coefficient of Sc^{3+} is underestimated with respect to the experimental one (see Table 3). This difference is partly due to the fact that the MCDHO2 water model underestimates D_{H_2O} with respect to the bulk water experimental one, 1.8 *vs* 2.3· 10^{-5} cm^2 s^{-1} [25], then Sc^{3+} aquaion is partially restrained by the low bulk water mobility.

Hydration enthalpy (ΔH_{hyd}) is fairly well estimated by the model, an underestimation smaller than 4% is observed in the worst case. It is interesting to note that

the main difference between the two developed intermolecular potentials is found in the energy, *POT*7 is 16 kcal/mol more stabilizing than *POT*6. Reexamining *POT*6//*POT*6 versus *POT*7//*POT*7 interaction energies in Table 1, one can verify that E_{int} gap is ~15 kcal/mol, roughly the same value found for ΔH_{hyd} gap. The information provided by Tables 1 and 3 allows us to make an energy decomposition of the hydration energy into two contributions. The first one corresponds to E_{int}, associated to $[Sc(H_2O)_6]^{3+}$ aquaion formation, −543 and −558 kcal/mol for *POT*6 and *POT*7, respectively. The second contribution corresponds to the hydration energy of the hexahydrated aquaion, which is computed as the difference between, ΔH_{hyd} and E_{int} of $[Sc(H_2O)_6]^{3+}$ plus the corresponding thermal corrections to deal with energies at the enthalpy level. Thus, the hydration enthalpy of Sc^{3+} hexahydrate is −368 and −370 kcal/mol, for *POT*6 and *POT*7, respectively. This energy decomposition tells us that more than 60% of the aquaion stability is due to the specific interactions inside the aquaion. Bulk contribution is greater than that corresponding to the classical Born term, for a triply charged sphere of 4 Å radius (~ − 190 kcal/mol), what indicates that important first–second hydration shell interactions still contribute to the whole hydration energy.

The information provided by Tables 1, 2 and 3 indicates that *POT*6 and *POT*7 are giving almost the same values for the physicochemical properties of the ion in solution except for the interaction energy, where a threshold of ~15 kcal/mol shifts one energy reference from the other. This *POT*6–*POT*7 shifting represents less than 2% of the mean ion-water interaction energy operating in the system.

Figure 3 displays the power spectra of the Sc (black line) and the first-shell oxygen (red line) velocity autocorrelation functions provided by the MD simulation. We will analyze the low-frequency part of the power spectrum, which is the region where the developed Sc–H_2O intermolecular potential is revealed. The results correspond to the simulation using *POT*6, similar spectra are obtained when using *POT*7 instead. The top of the figure presents spectra derived from a simulation of $[Sc(H_2O)_6]^{3+}$ cluster isolated at 300K. The blue lines denote the position of the quantum mechanical MP2 frequencies of the optimized Sc^{3+} hexahydrate corresponding to the more representative bending and stretching intermolecular modes. The hexahydrate power spectra present two peaks at low frequency, 115 and 180 cm^{-1} that can be associated to bending modes, whereas at higher frequencies three bands appear at 350–385, 460 and 510 cm^{-1}, which can be associated to the ScO stretching mode region. There is a parallelism with the QM frequencies with a blue shifting of ~50–70 cm^{-1}. This is due to

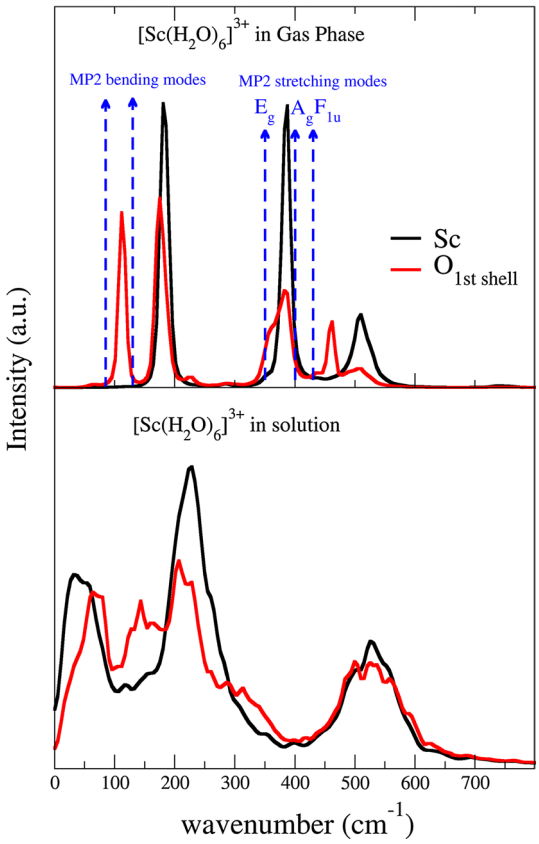

Fig. 3 Fourier transform of velocity autocorrelation functions (FT-VAC) of Sc^{3+} Aquaion for gas phase (*top*) and solution (*bottom*). (*blue arrows* correspond to representative quantum mechanical frequencies)

the difficulty of the intermolecular potential to reproduce the potential energy surface at the second derivative level. The shape of the potential energy surface in the region of one ScO stretching and OScO bending normal modes given by QM and *POT*6 is compared in the SM (Figures S7 and S8). It is shown that the *POT*6 curves do have curves leading to larger force constants and their associated frequencies. An analysis of correlation functions associated to dynamic variables of the hydrate internal geometrical parameters allows the assignment of the peak observed in the power spectra to several normal modes [18, 37]. Thus, 370 cm^{-1} broad band can be associated to E_g stretching mode, whereas 460 cm^{-1} peak is an A_g symmetric stretching mode. A final stretching mode, mixed with some bending moves, is centered at 510 cm^{-1}. When the aquaion is immersed in the solution, the power spectra change (bottom of Fig. 3): (i) A general broadening of the narrow bands observed in gas phase; (ii) the appearance of new bands due to the intermolecular bulk water interactions incorporated, this new band appearing in the 30–100 cm^{-1} region. The other two bands come from the convolution of the stretching and bending modes, whose

peak center is ~50 cm^{-1} blue-shifted with respect to gas phase. Rudolph and Pye [2] studied the vibrational spectra of a 1.65 M aqueous solution of $Sc(ClO_4)_3$ containing a perchloric acid excess to prevent hydrolysis of Sc^{3+} aquaion. Raman spectrum presents two bands, one of them depolarized (E_g) at 410 cm^{-1}, and the other one, polarized (A_{1g}) at 442 cm^{-1}, which corresponds to the stretching modes. A third vibrational IR active band (F_{1u}) is centered at 460 cm^{-1}, which may also by assigned to a ScO asymmetric stretching mode. Bearing in mind the 50–60 cm^{-1} blue shifting of our power spectra, these three bands are well recognized in the gas-phase spectra. Solution of the aquaion leads to convolution of the three bands in only one broad band containing all of them. It must be pointed out that the computed power spectrum does not include the IR and Raman intensity, this being the reason precluding the implicit deconvolution of the total vibrational power spectrum provided by the experimental use of IR and Raman spectroscopies.

3.3 EXAFS spectroscopy

Figure 4 shows the comparison between experimental k^2-weighted EXAFS [11] and the simulated ones obtained using the snapshots of the simulations carried out with *POT6*(blue line) or *POT7*(red line). The agreement is remarkable, particularly in the main range [3–10.5 $Å^{-1}$]. At higher k values, there is experimental noise, and the signal is distorted, although the main oscillation is roughly followed by the simulated ones. Regarding the *POT6–POT7* comparison, it is clear again that the structural description provided by the two developed potentials is almost the same. The fact that both spectra almost match is a sound test of the convergence of the structural result given the high sensitivity of EXAFS to the structural ensemble of Sc–O distances, coordination numbers and structural and dynamical disorder. The fairly good agreement strongly supports one option for the open question on Sc^{3+} hydration, i.e., Sc^{3+} aquaion is an hexahydrate. The angle distribution function (ADF) OScO derived from the MD trajectory is shown in SM (Figure S9). The distribution shows two well-defined peak centered at 90° and 180° with a ratio 4:1, respectively. This is just the expected distribution for an octahedron. Migliorati and D'Angelo [3] have recently published an study where a Sc–H_2O intermolecular potential was built to carry out classical MD simulations which resulted in an octa-coordination for Sc^{3+}. They simulated the EXAFS spectrum using a strategy similar to that here presented. They display in Figure 3 of their work [3] a good agreement with the experimental EXAFS spectrum, but in a k-range [5–10 $Å^{-1}$] shorter than the range shown in Fig. 4. The exclusion of this important low-k part of the spectrum explains the different final conclusion reached by these authors with respect to that here proposed.

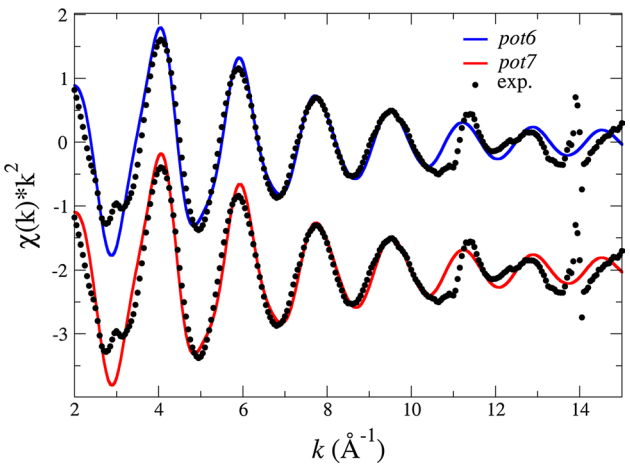

Fig. 4 Experimental k^2-weighted EXAFS (*dotted line*) versus two simulated spectra, each of them derived from the MD simulation using POT6 (*blue line*) or POT7 (*red line*)

4 Concluding remarks

This work has developed a modified version of the hydrated ion model to build highly charged metal cation–water intermolecular potentials and shown its good performance. The key-point of the new procedure is the combination of a polarizable and flexible water model (MCDHO2) and the explicit consideration of the ensemble of metal cation–water interactions present in a given aquaion, $[Sc(H_2O)_n]^{3+}$. Two intermolecular potentials have been built by fitting the MP2 interaction energies of $[Sc(H_2O)_6]^{3+}$ or $[Sc(H_2O)_7]^{3+}$ clusters. Only 40 structures have been needed to obtain reliable intermolecular potentials. This number could seem low for the usual sampling, but it must be pointing out that each structure considered in the sampling contains 6 or 7 Sc–H_2O interactions. Likewise, the polarizable character of the particles adds intrinsic ability to be well-adapted to non-explored arrangements. Both MD simulations supply the same structural and dynamical description of Sc^{3+} aqueous solution. The average Sc–O first-shell distance is 2.15 ± 0.01 Å and the hydration number is 6. The good agreement of the simulated vibrational power spectra and the EXAFS spectrum with the corresponding experimental information, together with the fair agreement of the computed hydration enthalpy, strongly support the developed potential, the new methodology, and the results derived from the MD simulation. The ion radius size invoked to expect a higher hydration number does not seem to be confirmed. Differing from some previous works [3, 5, 9] where hepta- or octa-coordinations were proposed for Sc^{3+}, we found a metal cation behavior

close to that of other small and hard trivalent cations, such as Cr^{3+} or Al^{3+}, in agreement with Rudolph and Pye [2] and the theoretical proposal of Rotzinger [10].

Acknowledgements We thank Prof. Persson for providing us with the original Sc *K*-edge EXAFS spectrum of Scandium aqueous solution published in Ref. [11]. We acknowledge the Spanish Junta de Andalucía for financial support (Proyecto de Excelencia, P11-FQM7607) and DZC for a predoctoral grant.

References

1. Cotton S (1999) Polyhedron 18(12)
2. Rudolph WW, Pye CC (2000) J Phys Chem A 104:1627
3. Migliorati V, D'Angelo P (2016) Inorg Chem 55:6703
4. Richens DT (1997) The chemistry of aqua ions. Wiley, Chichester
5. Kanno H, Yamaguchi T, Ohtaki H (1989) J Phys Chem 93:1695
6. Yamaguchi T, Niihara M, Takamuku T, Wakita H, Kanno H (1997) Chem Phys Lett 274:485
7. Smirnov P, Wakita H, Yamaguchi T (1998) J Phys Chem B 102:4802
8. Smirnov P, Trostin T (2011) Russ J Gen Chem 83(1):18
9. Vchirawongkwin V, Kritayakornupong C, Tongraar A, Rode BM (2012) Dalton Trans 41:11889
10. Rotzinger FP (1997) J Am Chem Soc 119:5230
11. Lindqvist-Reis P, Persson I, Sandström M (2006) Dalton Trans 28(32):3868
12. Sandström M, Persson I, Jalilehvand F, Lindqvist-Reis P, Spanberg D, Hermansson K (2001) J Synchrotron Rad 8:657
13. Abbasi A, Lindqvist-Reis P, Eriksson L, Sandström D, Lidin S, Persson I, Sandström M (2005) Chem Eur J 11:4065
14. Yamamoto T (2008) X-Ray Spectrom 37:572
15. Martínez JM, Torrico F, Pappalardo RR, Sánchez Marcos E (2004) J Phys Chem B 108:15851
16. Pappalardo RR, Sánchez Marcos E (1993) J Phys Chem 97:4500
17. Martínez JM, Pappalardo RR, Sánchez Marcos E (1998) J Chem Phys 109:1445
18. Martínez JM, Pappalardo RR, Sánchez Marcos E (1999). J Am Chem Soc 121:3175
19. Torrico F, Pappalardo RR, Sánchez Marcos E, Martínez JM (2006) Theor Chem Acc 115:196
20. Galbis E, Hernández-Cobos J, den Auwer C, Naour CL, Guillaumont D, Simoni E, Pappalardo RR, Sánchez Marcos E (2010) Angew Chem Int Ed 22:3811
21. Galbis E, Hernández-Cobos J, Pappalardo RR, Sánchez Marcos E (2014) J Chem Phys 140:214104
22. Saint-Martin H, Hernández-Cobos J, Bernal-Uruchurtu MI, Ortega-Blake I, Berendsen HJC (2000) J Chem Phys 113:10899
23. Morales N, Galbis E, Martínez JM, Pappalardo RR, Sánchez Marcos E (2016) J Phys Chem Lett 7:4275
24. Caralampio DZ, Martínez JM, Pappalardo RR, Sánchez Marcos E (2017) Submitted for publication
25. Villa A, Hess B, Saint-Martin H (2010) J Chem Phys 133:044509
26. Dolg M, Weding U, Stoll H, Preuss H (1987) J Chem Phys 86:866
27. Frisch MJ, Trucks GW, Schlegel HB, Scuseria GE, Robb MA, Cheeseman JR, Scalmani G, Barone V, Mennucci B, Petersson GA, Nakatsuji H, Caricato M, Li X, Hratchian HP, Izmaylov AF, Bloino J, Zheng G, Sonnenberg JL, Hada M, Ehara M, Toyota K, Fukuda R, Hasegawa J, Ishida M, Nakajima T, Honda Y, Kitao O, Nakai H, Vreven T, Montgomery JA, Peralta Jr JE, Ogliaro F, Bearpark M, Heyd JJ, Brothers E, Kudin KN, Staroverov VN, Kobayashi R, Normand J, Raghavachari K, Rendell A, Burant JC, Iyengar SS, Tomasi J, Cossi M, Rega N, Millam JM, Klene M, Knox JE, Cross JB, Bakken V, Adamo C, Jaramillo J, Gomperts R, Stratmann RE, Yazyev O, Austin AJ, Cammi R, Pomelli C, Ochterski JW, Martin RL, Morokuma K, Zakrzewski VG, Voth GA, Salvador P, Dannenberg JJ, Dapprich S, Daniels AD, Farkas Ö, Foresman JB, Ortiz JV, Cioslowski J, Fox DJ (2009) Gaussian 09 Revision D.01. Gaussian Inc. Wallingford CT
28. Smith W, Forester T, Todorov IT (2012) The dl_poly classic. STFC Daresbury Laboratory, Daresbury (UK)
29. Rehr JJ, Kas JJ, Vila FD, Prange MP, Jorissen K (2010) Phys Chem Chem Phys 12:5503
30. Merkling PJ, Muñoz-Páez A, Sánchez Marcos E (2002) J Am Chem Soc 124:10911
31. Carrera F, Torrico F, Richens DT, Muñoz-Paez A, Martínez JM, Pappalardo RR, Sánchez Marcos E (2007) J Phys Chem B 111:8223
32. Tomasi J, Mennucci B, Cammi R (2005) Chem Rev 105:2999
33. Terrier C, Vitorge P, Gaigeot MP, Spezia R, Vuilleumier R (2009) J Phys Chem B 113:7270
34. Helm L, Merbach A (2005) Chem Rev 105:1923
35. Marcus Y (2015) Ions in solution and their solvation. Wiley, New York
36. Helm L, Merbach A (1999) Coord Chem Rev 187:151
37. Irish DE, Brooker MH (1976) Advances in infrared and Raman spectoscopies. Heyden, vol 2, chap 6